Society of Medical Education & Research

2025, Volume 5, Issue 1, Page No: 80-92
ISSN: 3108-4826

Journal of Medical Sciences and Interdisciplinary Research

In Silico Identification of VKORC1 Antagonists from Celery Leaves (Apium graveolens L.) Using Molecular Docking and Dynamics

Noor Amira Hassan[1]*, Farah Nadia Rahman[1]

[1]Department of Management, Faculty of Business, University of Malaya, Kuala Lumpur, Malaysia.

***E-mail** ✉ amira.hassan.um@gmail.com

Abstract

The vitamin K cycle, particularly involving the enzyme VKORC1 (Vitamin K epoxide reductase complex subunit 1), plays a critical role in blood coagulation processes. Any interference with this cycle is often linked to vascular disorders, including myocardial infarction and stroke. Although warfarin is a widely prescribed anticoagulant, it carries risks due to interactions with many other medications, highlighting the need for safer alternatives. The ethanol extract of celery leaves (Apium graveolens L.) demonstrates promising anticoagulant effects, yet the specific active compound remains unidentified. Computer-aided drug design (CADD) techniques enable in silico prediction of compound interactions with target binding sites. This study sought to forecast binding interactions and identify stable complexes formed by compounds from the ethanol extract of celery leaves acting as VKORC1 antagonists. Twenty-three compounds were docked using AutoDock 4.2, followed by molecular dynamics simulation in AMBER 18 to evaluate the stability of the top five candidates. Docking results from 17 tested ligands identified five leading compounds: 6-isopentenyloxy-isobergapten (S1), Heratomin (S2), Apigenin (S3), Lanatin (S4), and Isoimperatorin (S5), with ΔG values of −9.27, −9.26, −9.22, −9.13, and −8.94 kcal/mol, respectively. Subsequent MD simulation over 100 ns confirmed 6-isopentenyloxy-isobergapten as the most effective ligand for maintaining complex stability among the five. In summary, 6-isopentenyloxy-isobergapten derived from celery leaves shows promise as a potential anticoagulant targeting VKORC1.

Keywords: Anticoagulants, Celery leaves, Molecular docking, Molecular dynamics, VKORC1

Introduction

Hemostasis refers to the rapid cessation of bleeding from damaged blood vessels, allowing blood flow to bypass the injured area and minimize loss during trauma. Coagulation, involving clot formation, is a key component of this process. Imbalances in hemostasis can lead to pathological conditions, such as uncontrolled bleeding due to failure of clot formation or excessive thrombosis, causing vessel occlusion [1]. Such thrombi contribute to vascular pathologies, including myocardial infarction, stroke, and related disorders. Cardiovascular diseases rank among the top global causes of mortality. In 2016, the World Health Organization (WHO) reported 56.9 million deaths from ischemic heart disease and 15.2 million from stroke [2]. Management involves both pharmacological and non-pharmacological approaches, with anticoagulants commonly employed to address thromboembolism-related vascular issues.

Anticoagulants are medications that inhibit clot formation by interfering with the conversion of fibrinogen to fibrin or by blocking clotting factors through calcium binding. They also help prevent embolus development and propagation [3]. Since 1954, warfarin, a vitamin K antagonist that blocks the synthesis of clotting factors VII, IX, X, and II, has been a leading anticoagulant, prescribed to 0.5–1.5% of the global population [4]. However, its narrow therapeutic window

Access this article online https://smerpub.com/

Received: 05 December 2024; **Accepted:** 17 March 2025

How to cite this article: Hassan NA, Rahman FN. In Silico Identification of VKORC1 Antagonists from Celery Leaves (Apium graveolens L.) Using Molecular Docking and Dynamics. J Med Sci Interdiscip Res. 2025;5(1):80-92. https://doi.org/10.51847/O6Bc56ujlU

and numerous drug interactions remain significant limitations [5]. This underscores the importance of developing alternative anticoagulant candidates with improved safety profiles.

Natural compounds from medicinal plants offer benefits, including accessibility, ease of isolation, and reduced adverse effects. Celery leaves (Apium graveolens L.) are valued in Indonesia not only as a culinary ingredient but also in traditional medicine. Prior studies indicate that celery possesses antidiuretic, antihypertensive, anti-inflammatory, antioxidant, antirheumatic, and anticoagulant activities. Its chemical constituents include flavonoids, saponins, tannins, essential oils, vitamins A, B, and C, asparagine, calcium, sulfur, and phosphorus, distributed throughout the plant [6]. Additional research has shown that ethanol extracts of celery leaves can substitute for EDTA as an anticoagulant in platelet counts [7]. At 50% concentration, the extract performed equivalently to EDTA. Further investigation into the specific bioactive components responsible for anticoagulant activity in celery is therefore warranted. Conventional discovery methods relying on bioassay-guided fractionation are labor-intensive and expensive.

This study is grounded in the hypothesis that phytochemicals from celery may disrupt VKORC1 function, thereby inhibiting the vitamin K cycle. Three-dimensional models of human VKORC1 and its enzymatic states have been described, with validated metastable structures providing insight into the reaction mechanism for vitamin K conversion [8]. Molecular docking and dynamics simulations serve as effective virtual screening and stability assessment tools to evaluate ligand-protein binding and facilitate target optimization [9–12].

The objective of this research was to examine the binding affinity, interaction profiles, and complex stability of compounds from celery leaves (Apium graveolens L.) with the VKORC1 enzyme structure as potential anticoagulant lead candidates. The process involved a literature review of plant-derived isolates, followed by molecular docking and dynamics simulations. Candidate leads were evaluated based on binding affinity (ΔG and Ki values), interaction modes, and MMGBSA analysis.

Materials and Methods

Computational hardware

All molecular docking and molecular dynamics (MD) simulations were conducted on a personal computer equipped with an AMD® Ryzen9 3900X CPU, Nvidia® GTX 1080 Ti GPU, 32 GB of RAM, and dual operating systems, Ubuntu 16.04 LTS and Windows 10 Pro 64-bit.

Ligand preparation and pharmacochemical analysis

This investigation utilized 23 bioactive compounds previously identified in celery leaves. The 3D structures of these compounds were retrieved in *.sdf format from the RCSB Protein Data Bank (PDB) via https://pubchem.ncbi.nlm.nih.gov/. The structures were then converted into *.pdb format using Discovery Studio 2016. To evaluate the drug-likeness of these compounds, Lipinski's Rule of Five was applied, analyzing parameters such as log P, molecular weight, hydrogen bond donors, hydrogen bond acceptors, and molar refractivity (MR).

VKORC1 protein preparation

The three-dimensional crystal structure of VKORC1 (PDB ID: 6WV3) was downloaded from the RCSB PDB (https://pubchem.ncbi.nlm.nih.gov/) in *.pdb format. Using Discovery Studio 2016, the protein structure was cleaned by removing the native ligand, water molecules, solvents, and any non-standard residues.

Validation of molecular docking

Docking protocol validation was performed by re-docking the native ligand (SWF) into the cleaned VKORC1 protein using AutoDock 4.2.6. The protein structure was prepared by adding polar hydrogens and charges and saved in *. pdbqt format. The native ligand was positioned at the center of the grid box, with its size adjusted accordingly. The Lamarckian Genetic Algorithm was used as the search method, performing 100 ns of GA runs with a medium number of maximum energy evaluations. The validation of the docking procedure was assessed using root-mean-square deviation (RMSD).

Docking of test ligands

The docking of the 23 test compounds was carried out using the validated docking parameters. All ligands in *.pdb format were converted to *.pdbqt format using AutoDock 4.2. Docking results were interpreted based on binding free energy (ΔG), inhibition constant (Ki), and visualization of interactions with VKORC1 amino acid residues.

Molecular dynamics simulation

MD simulations were executed using AMBER 18. Prior to the simulations, the best-docked conformation of each ligand was selected. The simulation protocol included protein and ligand preparation, topology and coordinate generation, energy minimization, heating, equilibration, production, and post-simulation analysis.

Protein-ligand complexes were solvated with water and neutralized by adding ions (Na^+, K^+, Ca^{2+}, Cl^-, H^+). Energy minimization was conducted in three steps: first, water molecules were minimized for 1000 steps; second, the entire system, including protein, ligand, and water, was minimized for 1000 steps; third, the full system topology was minimized.

The heating phase involved gradually increasing the temperature from 0–100 K, then 100–200 K, and finally to 200–310 K. Production simulations were performed for 100 ns after equilibration. The MD trajectories were analyzed using RMSD, RMSF, MM-GBSA binding free energy calculations, and energy decomposition analyses.

Results and Discussion

In silico drug design approaches are increasingly recognized as essential tools for the development of novel therapeutics and protein targets in biotechnology and pharmaceutical research. These computational bioinformatics techniques play a critical role in identifying molecular targets and predicting potential drug candidates for a wide range of human diseases [13]. In this context, the current study focused on screening phytochemical compounds from celery leaves against VKORC1 using molecular docking and molecular dynamics simulations to identify promising lead molecules.

VKORC1 three-dimensional structure

Vitamin K antagonists act as anticoagulants primarily by targeting vitamin K epoxide reductases (VKORC1), a group of integral membrane enzymes. The 3D crystal structure of VKORC1 (PDB ID 6WV3) consists of a 155-amino acid chain complexed with its native ligand (SWF) and OLC, and it also includes a water molecule [14]. The protein is derived from Homo sapiens, and its structure was resolved using X-ray diffraction at a resolution of 2.20 Å. Parameters critical for selecting suitable protein targets included method (X-ray diffraction), source organism (Homo sapiens), and resolution (<2 Å). Based on these criteria, VKORC1 (6WV3) was identified as the appropriate structure for docking. Only the cleaned form of the protein, devoid of non-standard residues, was employed for the docking simulations **(Figure 1a).**

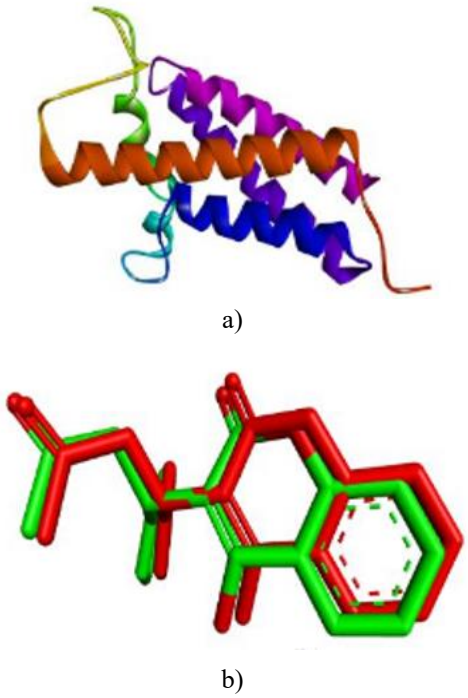

a)

b)

Figure 1. 3D representation of macromolecules and ligands: (a) VKORC1 protein (6WV3) structure; (b) superposition of the crystallized native ligand (SWF) and the best docking pose of the ligand.

Filtering of test ligands

The pharmacochemical characteristics of 23 celery-derived compounds were predicted using Lipinski's rule of five (http://www.scfbio-iitd.res.in/software/drugdesign/lipinski.jsp) to assess their potential for passive cell membrane permeation. According to Lipinski, orally active compounds should have: molecular weight <500 Da, Log P <5, ≤5 hydrogen bond donors, ≤10 hydrogen bond acceptors, and a molar refractivity (MR) range of 40–130.

Seventeen of the 23 compounds satisfied these oral drug-like criteria **(Table 1).** The six compounds S18, S19, S20, S21, S22, and S23 had negative Log P values, indicating poor lipophilicity and limited potential to penetrate the lipid bilayer. Conversely, compounds with Log P >5 are predicted to penetrate cell membranes more readily, potentially resulting in wider distribution and higher toxicity.

The BM (molecular weight) value also influenced predicted absorption: compounds S18, S20, S21, S22, and S23 exceeded 500 Da, suggesting limited diffusion through membranes. Similarly, the number of hydrogen bond donors and acceptors in S18, S19, S20, S21, S22, S23, and S10 suggested potential steric hindrance or strong binding, which may restrict interactions with the target binding site. Compounds S21, S22, and S23 additionally had MR values indicating possible weak or hindered interactions. Based on these criteria, the 17 compliant compounds were selected for further evaluation in molecular docking studies **(Table 1).**

Table 1. Physicochemical properties of the test ligands according to Lipinski's rule.

Entry	Test Ligand	Molecular Weight (Dalton)	Log P	Number of H-bond Donors	Number of H-bond Acceptors	MR (Molar Refractivity)	Ki (nM)	ΔG (kcal/mol)
S1	6-Isopentenyloxy-isobergapten	300	3.718	0	5	75.8089	0.161	-9.27
S2	Heratomin	270	3.709	0	4	82.3609	0.162	-9.26
S3	Apigenin	270	2.419	3	5	70.8138	0.175	-9.22
S4	Lanatin	270	3.709	0	4	75.8089	0.202	-9.13
S5	Isoimperatorin	270	3.709	0	4	75.8089	0.282	-8.94
S6	Oxypeucedanin	286	2.921	0	5	75.3299	0.348	-8.91
S7	Kaempferol	286	2.305	4	6	72.3856	0.319	-8.86
S8	Luteolin	286	2.125	4	6	72.4786	0.351	-8.81
S9	Imperatorin	270	3.709	0	4	75.8089	0.419	-8.70
S10	Quercetin	302	2.010	5	7	74.0504	0.465	-8.64
S11	Chrysoeriol	300	2.428	3	6	77.3658	0.694	-8.40
S12	γ-Selinene	204	4.869	0	0	66.8129	1.18	-8.09
S13	Δ-Selinene	204	4.869	0	0	66.8129	1.37	-8.00
S14	(S)-Rutaretin	262	1.398	2	5	67.1935	1.49	-7.95
S15	α-Selinene	204	4.725	0	0	66.7429	1.59	-7.91
S16	Apiumetin	244	2.204	1	4	65.7097	1.71	-7.87
S17	Osthenol	230	2.833	1	3	65.9107	1.97	-7.78
S18*	Luteolin 7-O-β-D-apiofuranosyl-β-D-glucopyranoside	580	-2.087	9	15	131.1621	-	-
S19*	Luteolin 7-O-β-D-glucopyranoside	448	-0.401	7	11	105.2090	-	-
S20*	Apigenin 7-O-β-D-apiofuranosyl(1→2)-β-D-glucopyranoside	564	-1.792	8	14	129.4973	-	-
S21*	Chrysoeriol 7-O-β-D-apiofuranosyl(1→2)-β-D-glucopyranoside	594	-1.784	8	15	136.0493	-	-
S22*	Luteolin 7-O-[β-D-apiofuranosyl(1→2)-(6″-O-malonyl)]-β-D-glucopyranoside	666	-2.061	9	18	147.2882	-	-
S23*	Apigenin 7-O-[β-D-apiofuranosyl(1→2)-(6″-O-malonyl)]-β-D-glucopyranoside	650	-1.767	8	17	145.6234	-	-

Note: Molecular docking simulations were not performed for compounds excluded by Lipinski criteria.

Validation of the molecular docking process

To ensure the reliability of the docking methodology, the native ligand was re-docked into its macromolecular target. The purpose of this validation was to confirm the native ligand's binding site and establish accurate parameters for subsequent docking of the test compounds. Docking validation was considered acceptable when the RMSD (Root Mean Square Deviation) was ≤2 Å, indicating minimal deviation and suitability for simulation. The grid box coordinates and dimensions were set as X = −10.742, Y = 27.718, Z = 55.762, with box size 50 × 42 × 44. Additional parameters included a grid spacing of 0.375 Å and the Lamarckian Genetic Algorithm as the search method. Docking conformations were sampled 100 times with medium energy evaluation. The best pose of the native ligand **(Figure 1b)** showed a ΔG of −10.91 kcal/mol, Ki of 0.452 nM, and RMSD of 0.45 Å, confirming that the chosen grid parameters were suitable for docking the test ligands.

Ligand interactions with VKORC1

Docking scores were used to evaluate binding affinities and predict preferred interaction sites. Results were expressed as binding free energies (ΔG), inhibition constants (Ki), and detailed interaction patterns between the ligands and VKORC1 **(Table 1 and Figure 2).** Lower ΔG values indicate stronger ligand-protein interactions, while Ki reflects the binding affinity [15]. Interactions were visualized through hydrogen bonds, van der Waals forces, and hydrophobic contacts such as pi-alkyl, alkyl, and pi-sigma. Amino acids ASN80 and TYR139 played key roles in potential anticoagulant activity [16].

For the native ligand SWF, 19 amino acids within the VKORC1 active site participated in interactions, forming three hydrogen bonds with ASN80, TYR139, and GLY60, in addition to van der Waals and hydrophobic interactions **(Figure 2).** All test ligands were able to bind to the VKORC1 active site (ΔG < 0), with each forming interactions with TYR139 and ASN80. However, none exhibited stronger ΔG or Ki than the native ligand. The ligands with the lowest ΔG and Ki—S1, S2, S3, S4, and S5—were selected for further molecular dynamics simulations to evaluate complex stability.

Complex stability of VKORC1-ligand interactions

MD simulations were performed on the VKORC1 protein in complex with the native ligand and the top five test ligands (S1–S5) to assess structural stability over time. AMBER 18 was used to run 100 ns simulations, with analyses of RMSD, RMSF, MM-GBSA, MMPBSA, and energy decomposition.

RMSD

Root mean square deviation (RMSD) is commonly used in three-dimensional molecular studies to quantify conformational changes of a molecule over time. RMSD analysis was conducted to verify that the protein-ligand complexes remained structurally stable throughout the simulation and to assess the extent of positional changes of the ligands from the start to the end of the simulation.

For the native ligand, RMSD analysis showed that its conformation remained largely stable during the entire simulation without any major fluctuations. The protein itself maintained a stable conformation from 0 ns until around 35 ns. At 48 ns, a transient spike in RMSD was observed, after which it gradually returned to baseline and remained steady until the simulation concluded.

Among the test ligands, S1 and S2 displayed similar RMSD profiles throughout the simulation, suggesting that both ligands preserved stable conformations without significant deviations. The protein also retained its structural integrity during these simulations.

Ligand S3 exhibited a positional shift after 20 ns, maintaining this new conformation until the simulation ended, with an RMSD of approximately 1 Å. During the initial 5 ns, the protein RMSD rose to 2.5 Å and then stabilized, with only minor changes observed towards the end. Ligand S4 remained stable initially, experienced a spike at 44 ns, and then remained steady; the protein showed slight instability at 10 ns, stabilized until 90 ns, and spiked again at the end of the simulation. Ligand S5 demonstrated consistent RMSD throughout the simulation, and the protein also remained stable for the duration of the run.

Overall, RMSD values for all five test ligands were below 2 Å, while RMSD values for the protein were under 5 Å **(Figure 3).** These observations indicate that all test ligands, together with the native ligand, effectively maintained the stability of the protein-ligand complexes.

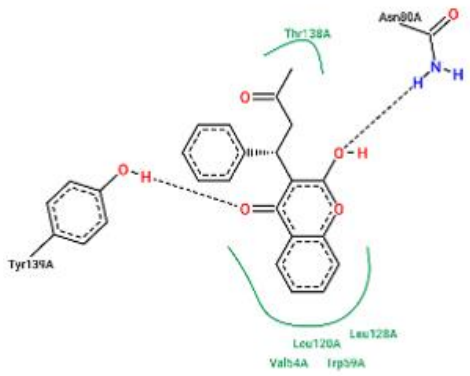

SWF

a)

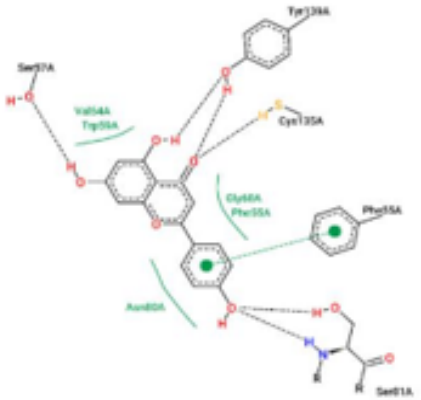

S3

d)

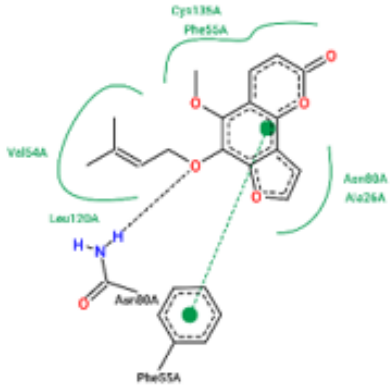

S1

b)

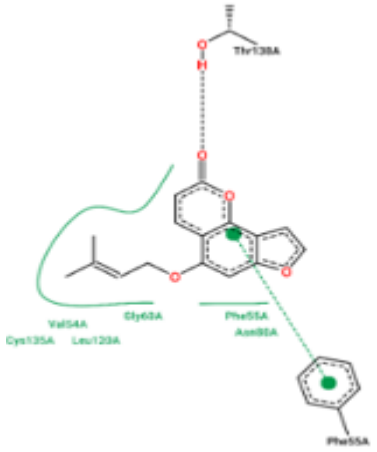

S4

e)

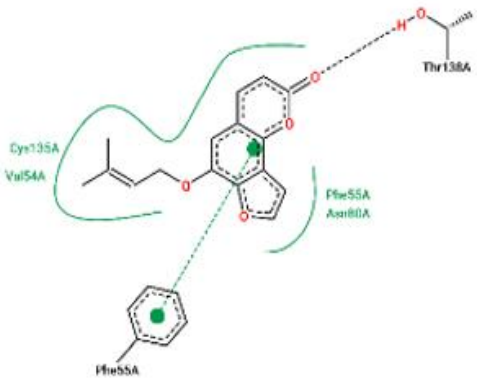

S2

c)

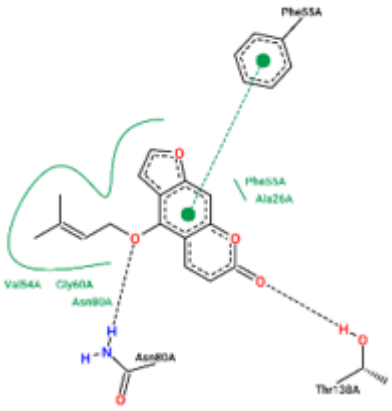

S5

f)

Figure 2. Representative 2D depiction of ligand interactions within the VKORC1 protein binding site.

RMSF analysis

The root mean square fluctuation (RMSF) measures the deviation of a particle's position relative to a reference point, expressed as a square root. RMSF was calculated for each C-alpha residue to assess the extent of motion of amino acids during the simulation [14]. Regions with higher RMSF values indicate flexible residues. Helical protein regions containing flexible residues are less constrained by hydrogen bonds, allowing more freedom of movement. RMSF values for all ligands at the key residues Asn80 and Tyr139 ranged between 0.58–1.07 Å and 0.60–0.64 Å, respectively **(Figure 4).** Other residues, including 35, 47, 70, 100, and 127, exhibited RMSF values averaging 2.2, 2.2, 4, 2, and 3 Å, respectively. These fluctuations are not critical for complex stability, which depends primarily on Asn80 and Tyr139. Overall, RMSF < 2.0 Å at critical residues confirms that all ligands maintained stable positioning.

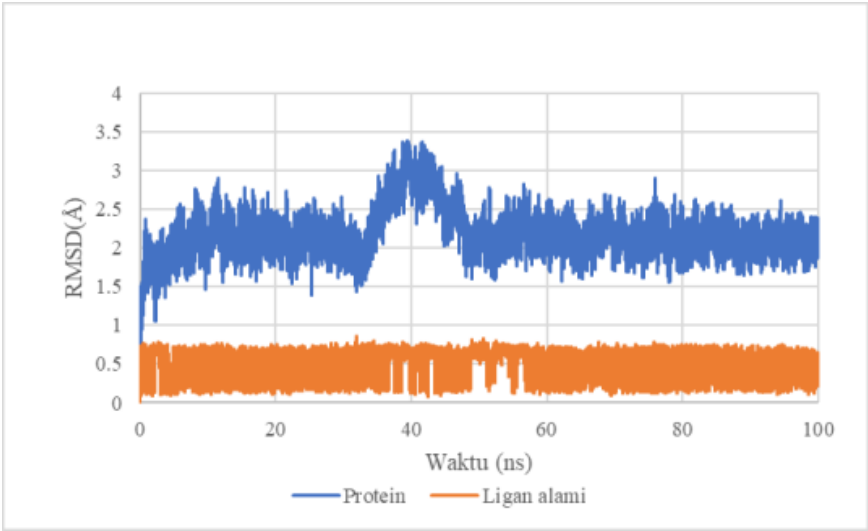

a)

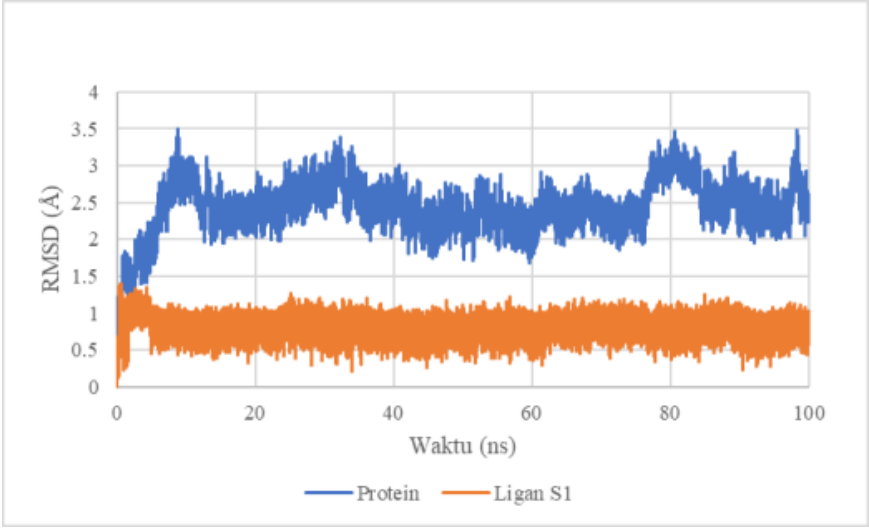

b)

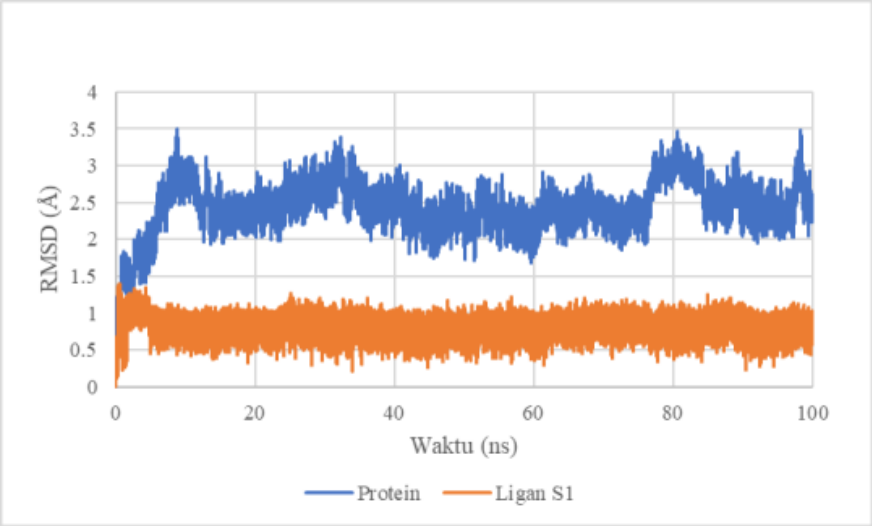
RMSD (Å)
Waktu (ns)
Protein
Ligan S1

c)

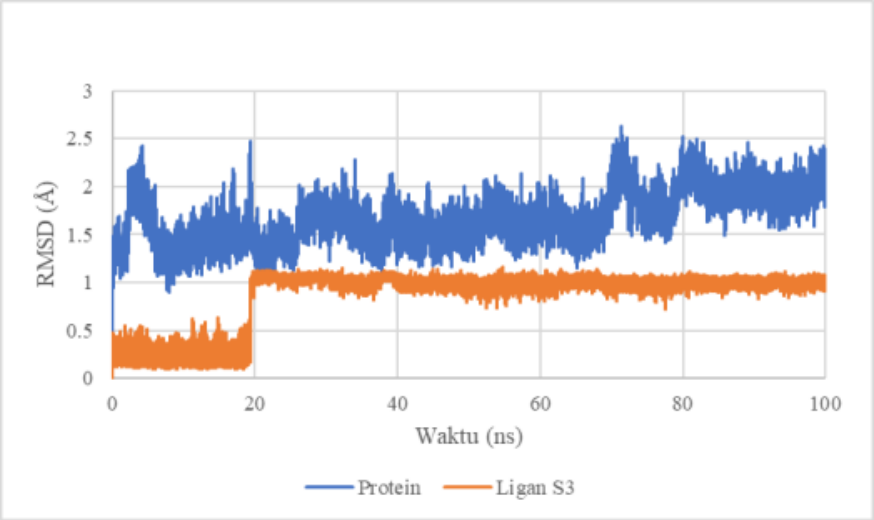
RMSD (Å)
Waktu (ns)
Protein
Ligan S3

d)

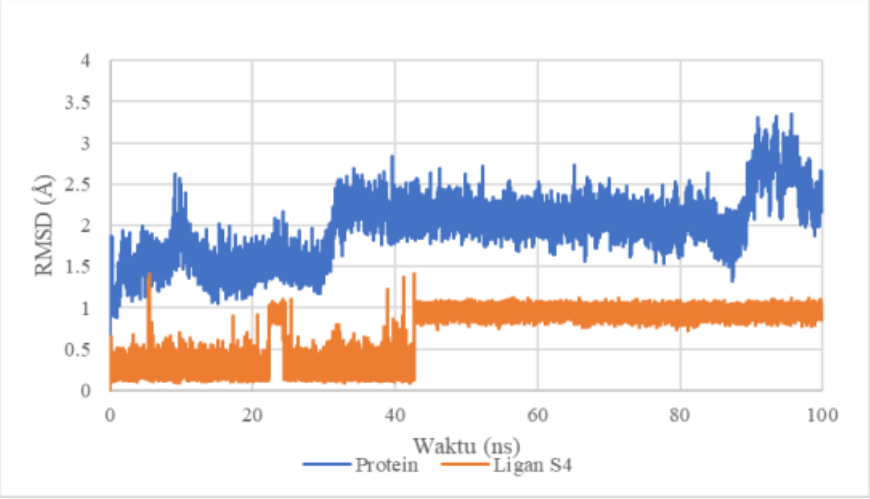
RMSD (Å)
Waktu (ns)
Protein
Ligan S4

e)

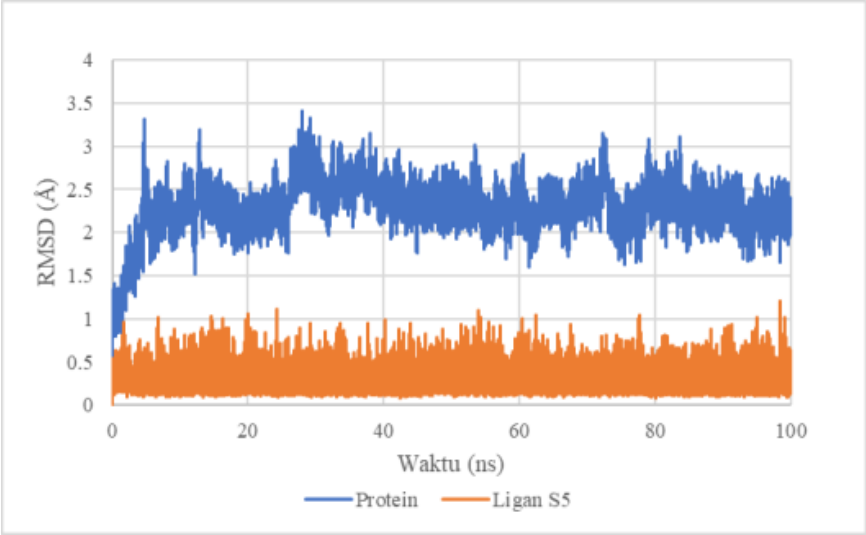

f)

Figure 3. RMSD variations of native and test ligands. a) SWF, b) S1, c) S2, d) S3, e) S4, f) S5

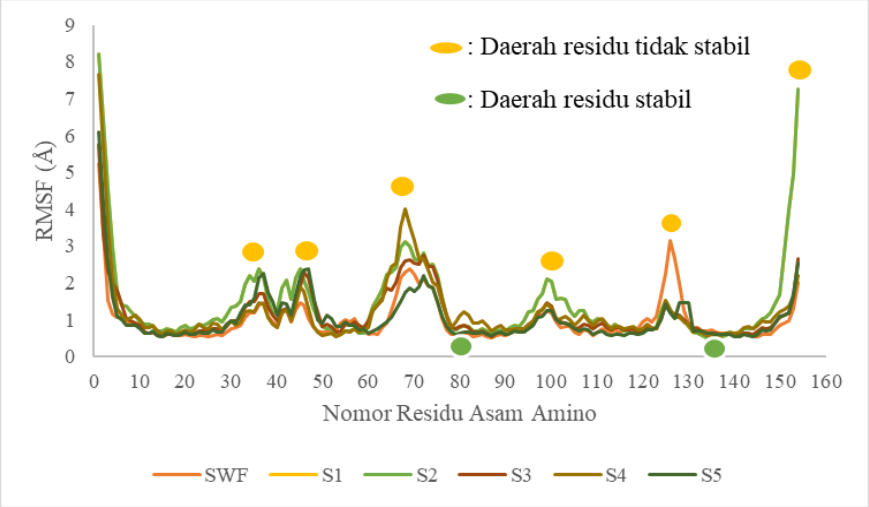

Figure 4. Residue fluctuations surrounding the binding atoms.

Quantification of hydrogen bonds

Hydrogen bonds occur between a hydrogen atom of one molecule and an electronegative atom such as nitrogen, oxygen, or fluorine in another molecule, representing one of the strongest dipole-dipole interactions [17]. The fraction of conformational residues that participate in at least one hydrogen bond during the simulation is termed hydrogen bond occupancy.

Analysis of hydrogen bond occupancy for the native ligand indicated that the highest occupancy was at Asn79, acting as a donor, with a value of 0.29%. Ligand S1 exhibited its maximum occupancy at Ala25 (donor) with 39.67%, while S2 showed the highest occupancy at Asn79 (donor) with 7.92%. Ligand S3 reached the highest occupancy at Ser56 (acceptor) with 72.47%. For S4, the maximum occupancy occurred at Asn79 (donor) with 1.72%, and ligand S5 showed the highest occupancy at Ser80 (donor) with 0.83%. Hydrogen bonds were considered strong if occupancy was ≥ 80% and stable if occupancy was ≥ 50% [18].

These results indicate that ligand S3 formed stable hydrogen bonds throughout the molecular dynamics simulation **(Figure 5).** This finding aligns with the molecular docking results **(Figure 2)**, which also highlighted stable hydrogen bond interactions in the S3 complex. The analysis suggests that there was significant

dynamic movement between the ligand and the protein during the simulation [10, 19].

MMGBSA

MMGBSA is a widely used computational approach for estimating the binding free energy between macromolecules and ligands [20]. The MMGBSA calculations are composed of several energy components, including van der Waals energy (EVDW), electrostatic energy (EEL), electrostatic contribution to solvation free energy (EGB), non-polar contribution to solvation free energy (ESURF), ΔG_gas, ΔG_solv, and the overall binding free energy (ΔG_total). A more negative ΔG_total indicates a stronger binding affinity of the ligand to the protein.

Van der Waals interactions (EVDW) were a major contributor to the MMGBSA binding energy for all ligands. For the native ligand (SWF), EVDW was calculated as -49.0176 kcal/mol, whereas ligand S1 exhibited a slightly less negative EVDW of -44.6267 kcal/mol. Non-covalent interactions, including van der Waals and electrostatic forces, are crucial for determining the overall binding affinity and the conformational stability of protein-ligand complexes, which are relevant in drug design, protein engineering, and even charge-transfer phenomena in optoelectronic systems [21].

Interestingly, ligand S3 showed the highest (most positive) EVDW but the most negative EEL, with a value of -19,859 kcal/mol. When considering the total binding energy, ligand S1 exhibited the most negative ΔG_total at -43.7432 kcal/mol **(Figure 6)**, indicating that S1 is capable of forming a more stable complex with VKORC1 compared to the native ligand.

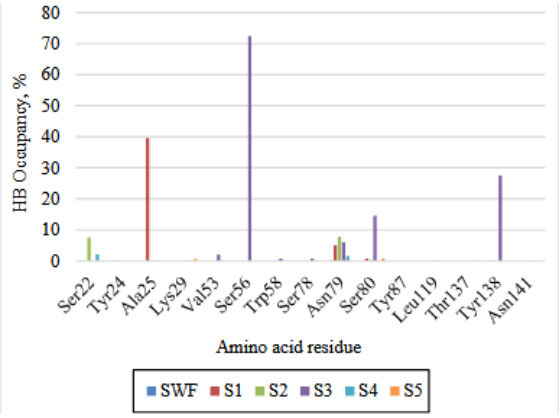

Figure 5. Hydrogen bond occupancy analysis.

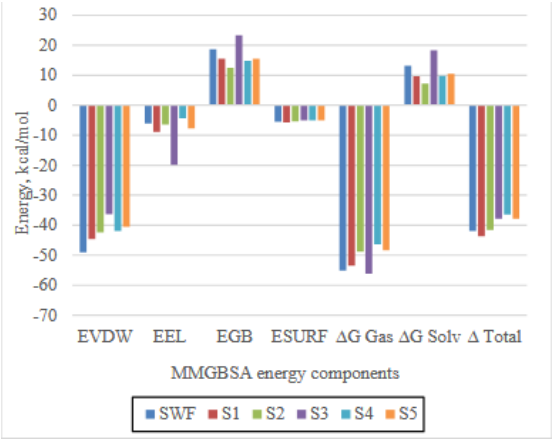

Figure 6. Component-wise MM-GBSA energy of ligand-protein complexes.

Decomposition

Decomposition analysis was conducted using the MMGBSA approach to determine which amino acid residues contribute most significantly to the binding between the protein and ligands [21]. For the native ligand (SWF), intermolecular interactions were observed with residues Leu21, Ser22, Ala25, Val53, Phe54, Phe62, Phe82, Phe86, Tyr87, Leu119, Val133, Asn79, Ser80, and Tyr137. Ligand S1 formed interactions with Ser22, Tyr24, Ala25, Val53, Phe54, Trp58, Gly59, Ser78, Asn79, Ser80, Leu119, Ile122, Leu123, Val133, Cys134, Thr137, and Tyr138. Ligand S2 interacted with residues Leu119, Ile122, Leu123, Cys134, Thr137, Ser22, Ala25, Val53, Phe54, Ser56, Trp58, Gly59, Phe62, Asn79, Ser80, and Leu119.

For ligand S3, the interacting residues included Ala25, Leu26, Lys29, Val53, Phe54, Ser56, Trp58, Gly59, Ser78, Asn79, Ser80, Leu119, Leu123, Cys134, and Tyr138. Ligand S4 formed bonds with Ala25, Lys29, Val53, Phe54, Ser56, Trp58, Gly59, Asn79, Ser80, Leu119, Ile122, Leu123, and Cys134. Similarly, ligand S5 engaged the same residues as S4. Across all five ligands, the Asn80 and Tyr139 residues consistently contributed to the interactions **(Figure 7),** demonstrating that the ligands maintained their initial binding positions observed in the MD simulations.

Molecular dynamics analysis confirmed satisfactory RMSD stability for all five complexes (S1–S5). RMSF analysis indicated that residues at the active site, specifically Asn80 and Tyr139, remained stable with RMSF values below 2 Å. Hydrogen bond analysis revealed that the S3 complex was the most stable, with a maximum occupancy of 72.47% at Ser56. MMGBSA

calculations identified complex S1 as having the most favorable binding affinity, with a total binding energy (ΔG) of -43.7432 kcal/mol. Overall, decomposition results indicated that complexes S1, S2, and S3 were stable, as they maintained interactions consistent with the molecular dynamics outcomes. S1 was selected as the lead compound due to its ability to preserve complex stability during the simulations, highlighting its potential as a candidate anticoagulant.

Conclusion

Among the 17 compounds tested, the five ligands S1, S2, S3, S4, and S5, with ΔG values of −9.27, −9.26, −9.22, −9.13, and −8.94 kcal/mol, respectively, demonstrated the strongest interactions with VKORC1. MD simulations over 100 ns showed that all five complexes maintained stable RMSD and RMSF profiles. Ligand S1 (6-isopentenyloxy-isobergapten) exhibited the lowest MM-GBSA total free energy (ΔG = −43.7432 kcal/mol), highlighting its potential as a lead compound for further development.

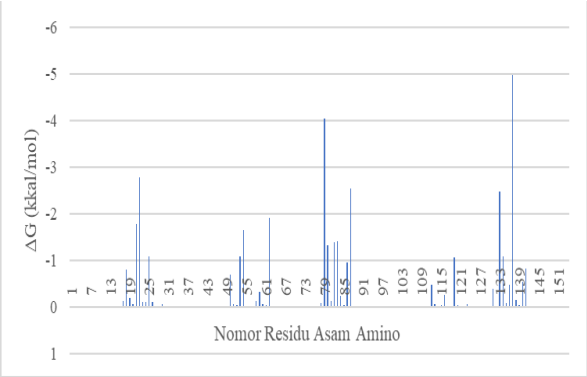

a)

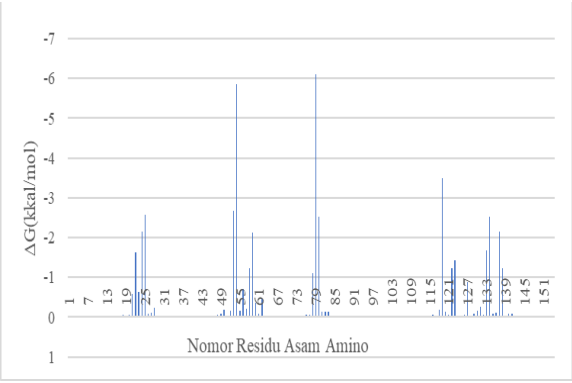

b)

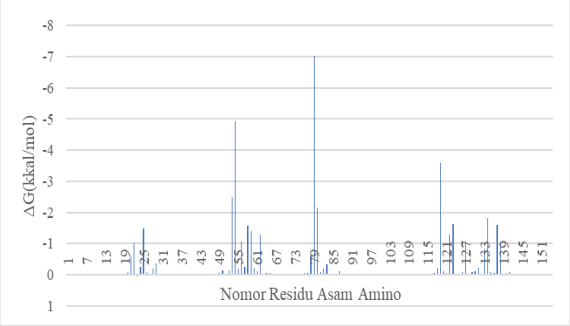

c)

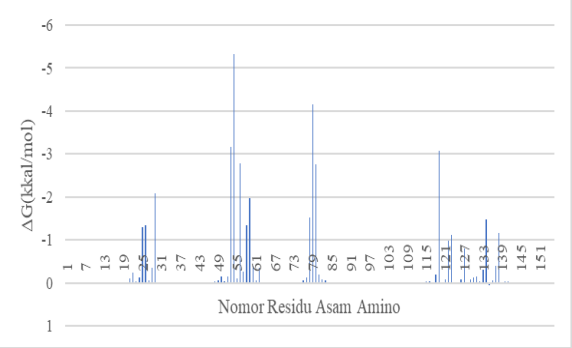

d)

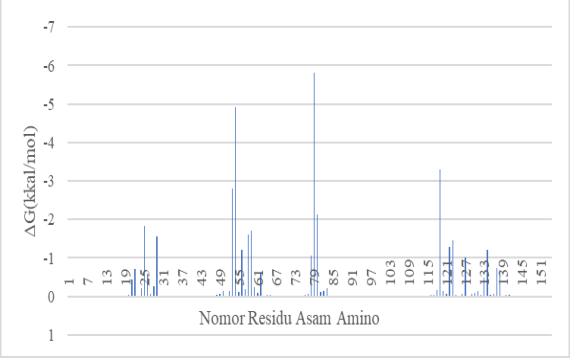

e)

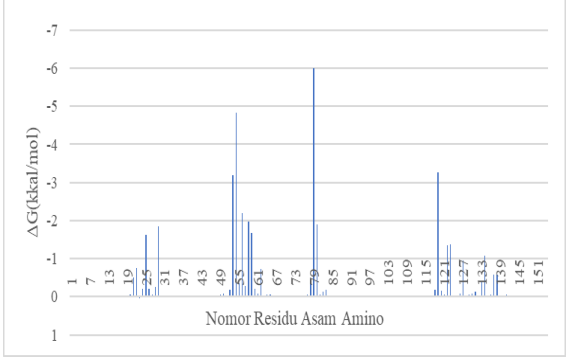

f)

Figure 7. Decomposition energy plot of the ligand-protein complexes. a) SWF, b) S1, c) S2, d) S3, e) S4, f) S5

Acknowledgments: None

Conflict of Interest: None

Financial Support: None

Ethics Statement: None

References

1. Saner FH, Kirchner C. Monitoring and Treatment of Coagulation Disorders in End-Stage Liver Disease. Visc Med. 2016;32(4):241-248. doi:10.1159/000446304
2. Laslett LJ, Alagona P, Clark BA, Drozda JP, Saldivar F, Wilson SR, Poe C, Hart M. The worldwide environment of cardiovascular disease: Prevalence, diagnosis, therapy, and policy issues: A report from the american college of cardiology. J Am Coll Cardiol. 2012;60(25 SUPPL.). doi:10.1016/J.JACC.2012.11.002
3. Gbyli R, Mercaldi A, Sundaram H, Amoako KA. Achieving Totally Local Anticoagulation on Blood Contacting Devices. Adv Mater Interfaces. 2018;5(4):1700954. doi:10.1002/ADMI.201700954
4. Johnson JA, Gong L, Whirl-Carrillo M, Gage BF, Scott SA, Stein CM, Anderson JL, Kimmel SE, Lee MTM,Pirmohamed M, Wadelius M, Klein TE, Altman RB. Clinical pharmacogenetics implementation consortium guidelines for CYP2C9 and VKORC1 genotypes and warfarin dosing. Clin Pharmacol Ther. 2011;90(4):625-629. doi:10.1038/clpt.2011.185
5. Sikka P, Bindra VK. Newer antithrombotic drugs. Indian J Crit Care Med. 2010;14(4):188-195. doi:10.4103/0972-5229.76083
6. Guven H, Arici A, Simsek O. Flavonoids in our foods: a short review. J Basic Clin Heal Sci. 2019;3(2):96-106.
7. Rumpho ME, Edwards GE, Loescher WH. A Pathway for Photosynthetic Carbon Flow to Mannitol in Celery Leaves. *Plant Physiol*. 1983;73(4):869-873. doi:10.1104/PP.73.4.869
8. Chatron N, Chalmond B, Trouvé A, Benoit E, Caruel H, Lattard V, Tchertanov L. Identification of the functional states of human Vitamin K epoxide reductase from molecular dynamics simulations. RSC Adv. 2017;7(82):52071-52090. doi:10.1039/C7RA07463H
9. Nursamsiar, Nur S, Febrina E, Asnawi A, Syafiie S. Synthesis and Inhibitory Activity of Curculigoside A Derivatives as Potential Anti-Diabetic Agents with β-Cell Apoptosis. J Mol Struct. 2022;1265. doi:10.1016/J.MOLSTRUC.2022.133292
10. Asnawi A, Aman LO, Nursamsiar, Febrina E. Molecular Docking and Molecular Dynamic Studies: Screening Phytochemicals of Acalypha Indica Against Braf Kinase Receptors For Potential Use In Melanocytic Tumours. Rasayan J Chem. 2022;15(2):1352-1361. doi:10.31788/RJC.2022.1526769
11. Febrina E, Asnawi A, Abdulah R, Lestari K, Supratman U. Identification of Flavonoids From Acalypha Indica L. (Euphorbiaceae) as Caspase-3 Activators Using Molecular Docking and Molecular Dynamics. Int J Appl Pharm. 2022;14(Special issue 5):162-166. doi:10.22159/IJAP.2022.V14S5.34
12. Ischak NI, Ode LA, Hasan H, Kilo A La, Asnawi A. In silico screening of Andrographis paniculata secondary metabolites as anti-diabetes mellitus through PDE9 inhibition. Res Pharm Sci. 2023;18(1):100. doi:10.4103/1735-5362.363619
13. Ritchie TJ, McLay IM. Should medicinal chemists do molecular modelling? Drug Discov Today. 2012;17(11-12):534-537. doi:10.1016/J.DRUDIS.2012.01.005
14. Liu S, Li S, Shen G, Sukumar N, Krezel AM, Li W. Structural basis of antagonizing the vitamin K catalytic cycle for anticoagulation. Science *(80-)*. 2021;371(6524). doi:10.1126/SCIENCE.ABC5667
15. Nursamsiar, Asnawi A, Kartasasmita RE, Ibrahim S, Tjahjono DH. Synthesis, biological evaluation, and docking analysis of methyl hydroquinone and bromo methyl hydroquinone as potent cyclooxygenase (COX-1 and COX-2) inhibitors. J Appl Pharm Sci. 2018;8(7):16-20. doi:10.7324/JAPS.2018.8703
16. Wu S, Chen X, Jin DY, Stafford DW, Pedersen LG, Tie JK. Warfarin and vitamin K epoxide reductase: a molecular accounting for observed inhibition. Blood. 2018;132(6):647. doi:10.1182/BLOOD-2018-01- 830901
17. Weinhold F, Klein RA. What is a hydrogen bond? Resonance covalency in the supramolecular domain. Chem Educ Res Pract. 2014;15(3):276-285. doi:10.1039/C4RP00030G
18. Cetin E, Atilgan AR, Atilgan C. DHFR Mutants Modulate Their Synchronized Dynamics with the

Substrate by Shifting Hydrogen Bond Occupancies. J Chem Inf Model. Published online December 26, 2022. doi:10.1021/acs.jcim.2c00507

19. Xie H, Li Y, Yu F, Xie X, Qiu K, Fu J. An investigation of molecular docking and molecular dynamic simulation on imidazopyridines as B-raf kinase inhibitors. Int J Mol Sci. 2015;16(11):27350-27361. doi:10.3390/ijms161126026
20. Genheden S, Ryde U. The MM/PBSA and MM/GBSA methods to estimate ligand-binding affinities. Expert Opin Drug Discov. 2015;10(5):449-461. doi:10.1517/17460441.2015.1032936
21. Mahmudov KT, Kopylovich MN, Guedes da Silva MFC, Pombeiro AJL. Non-covalent interactions in the synthesis of coordination compounds: Recent advances. Coord Chem Rev. 2017;345:54-72. doi:10.1016/J.CCR.2016.09.002